Multiplex protein assays based on real-time magnetic nanotag sensing

Sebastian J. Osterfeld[a,1], Heng Yu[b,1], Richard S. Gaster[c], Stefano Caramuta[b], Liang Xu[a], Shu-Jen Han[a], Drew A. Hall[d], Robert J. Wilson[a], Shouheng Sun[e], Robert L. White[a,d], Ronald W. Davis[b,2], Nader Pourmand[b,f,2], and Shan X. Wang[a,d,2]

[a]Departments of Materials Science and Engineering, [c]Bioengineering, and [d]Electrical Engineering, Stanford University, Stanford, CA 94305; [b]Stanford Genome Technology Center, Stanford University, Palo Alto, CA 94304; [e]Department of Chemistry, Brown University, Providence, RI 02912; and [f]Biomolecular Engineering, University of California, 1156 High Street, Santa Cruz, CA 95064

Contributed by Ronald W. Davis, October 28, 2008 (sent for review September 29, 2008)

Magnetic nanotags (MNTs) are a promising alternative to fluorescent labels in biomolecular detection assays, because minute quantities of MNTs can be detected with inexpensive giant magnetoresistive (GMR) sensors, such as spin valve (SV) sensors. However, translating this promise into easy to use and multilplexed protein assays, which are highly sought after in molecular diagnostics such as cancer diagnosis and treatment monitoring, has been challenging. Here, we demonstrate *multiplex* protein detection of potential cancer markers at subpicomolar concentration levels and with a dynamic range of more than four decades. With the addition of nanotag amplification, the analytic sensitivity extends into the low fM concentration range. The multianalyte ability, sensitivity, scalability, and ease of use of the MNT-based protein assay technology make it a strong contender for versatile and portable molecular diagnostics in both research and clinical settings.

giant magnetoresistive sensors | GMR | magnetic nanotags | multiplex protein detection | biochip

A consensus is emerging that early detection and personalized treatment in clinics based on genetic and proteomic profiles of perhaps 4–20 biomarkers are the key to improving the survival rate of patients with complex diseases, such as cancer, autoimmune disorders, infectious diseases, and cardiovascular diseases (1–3). Although the tools for large-scale biomarker discovery with hundreds to thousands of biomarkers are available, there are few biomolecular detection tools capable of multiplex and sensitive detection of protein biomarkers that can be readily adopted in clinical settings for biomarker validation and for personalized diagnosis and treatment. This need, we believe, can be fulfilled by the magnetic nanotag (MNT)-based biomolecular assay technology reported here. We demonstrate the feasibility and implementation of this technology with multiple potential cancer markers.

Several research groups are investigating MNT (4–6)-based analyte quantification as a highly sensitive alternative to optical biosensors and biochips (7–10). By labeling the target analyte of interest with MNTs (see Fig. 1), analyte detection and quantification can occur when the analyte binds to capture probes on the surface of giant magnetoresistive (GMR) sensors (11–15) such as spin valve (SV) sensors (16), which have been developed and optimized for use in hard disk drives on a scale of hundreds of millions of units annually with great economy and reliability. Such sensors, when modified for use in biological applications, were previously shown to be capable of detecting as few as 10 MNTs (13, 16).

Results

Given the recent efforts to develop methods for early cancer detection via quantification of cancer-related cytokines, we chose the following analytes for our MNT-based protein assays: cancer embryonic antigen (CEA), eotaxin, granulocyte colony-stimulating factor (G-CSF), interleukin-1-alpha (IL-1α), interleukin-10 (IL-10), IFN gamma (IFN-γ), lactoferrin, and tumor necrosis factor alpha (TNF-α). Fig. 1 outlines the detection scheme in which analyte is captured on the sensor surface and quantified with streptavidin-coated MNTs. Typically, the analyte and linker antibody incubation time (Fig. 1 *B* and *C*) is 1 h or less, whereas the MNT-based quantification (Fig. 1*D*) requires <15 min. It is possible to reduce the total assay time to <30 min, for example through analyte incubation in a microfluidic channel (17), so that it is suitable for physician office laboratory or point of care applications. We currently implement the MNT detection scheme on a custom fabricated chip, which has an array of 64 SV sensors and a 200-μl reaction well placed on top [see Supporting Information (SI)], so that the reagents can be pipetted and aspirated easily. At present, our prototype electronic instrumentation (see methods) is able to record up to 64 sensors in

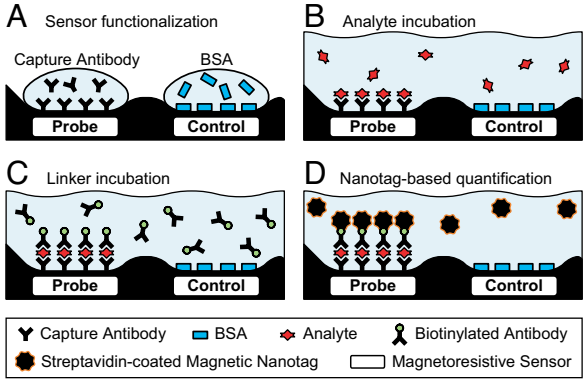

Fig. 1. Magnetic nanotag-based protein detection assay. Probe sensors are functionalized with capture antibodies specific to the chosen analyte, whereas control sensors are blocked with a 1 wt% BSA solution (*A*). During analyte incubation, the probe sensors capture a fraction of the analyte molecules (*B*). A biotinylated linker antibody is subsequently incubated, which binds to the captured analyte (*C*), and which provides binding sites for the streptavidin-coated magnetic nanotags. Streptavidin-coated magnetic nanotags are then incubated (*D*), and the nanotag binding signal, which saturates at an analyte concentration-dependent level, is used to quantify the analyte concentration.

Author contributions: S.J.O., H.Y., N.P., and S.X.W. designed research; S.J.O., H.Y., R.S.G., S.C., and L.X. performed research; S.J.O., H.Y., S.-J.H., D.A.H., R.J.W., S.S., and N.P. contributed new reagents/analytic tools; S.J.O., H.Y., R.L.W., R.W.D., N.P., and S.X.W. analyzed data; and S.J.O., H.Y., N.P., and S.X.W. wrote the paper.

Conflict of interest statement: Stanford University has licensed the magnetic bioassay chip technology described in this work to MagArray, Inc. S.J.O., H.Y., S.S., R.L.W., R.W.D., N.P., and S.X.W. hold financial interests in MagArray, Inc., in the form of stocks and stock options.

Freely available online through the PNAS open access option.

[1]S.J.O. and H.Y. contributed equally to this work.

[2]To whom correspondence may be addressed. E-mail: dbowe@stanford.edu, pourmand@soe.ucsc.edu, or sxwang@stanford.edu.

This article contains supporting information online at www.pnas.org/cgi/content/full/0810822105/DCSupplemental.

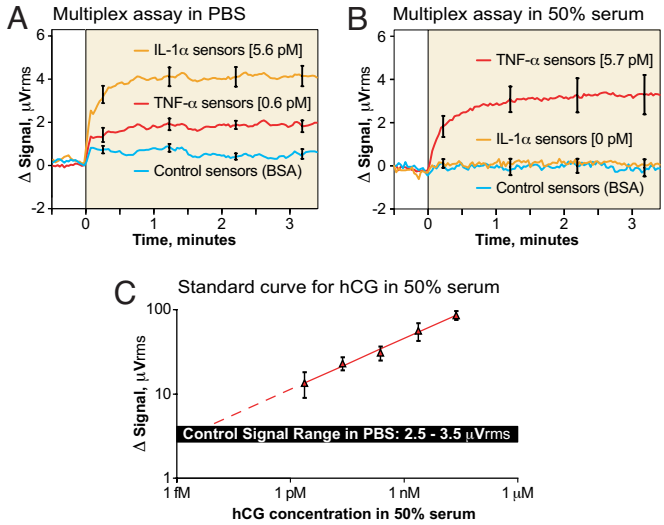

Fig. 2. Results. The average signal ± 1 S.D. is shown. In one experiment (*A*), 14 sensors on a chip were functionalized as follows: four sensors anti-IL-1α, eight sensors anti-TNF-α, two sensors BSA. A sample consisting of 5.6 pM IL1-α and 0.6 pM TNF-α in PBS was then incubated for 1 h. The time t = 0 defines the moment of nanotag application in the final step of the assay. In a comparable experiment (*B*), a second chip was similarly functionalized: five sensors anti-TNF-α, two sensors anti-IL-1α, two sensors BSA. However, this time the sample consisted of zero IL-1a and 5.7 pM TNF-α in 50% serum, balance PBS. Thus, both the sensors blocked with BSA and the IL-1α sensors were negative controls. In a third experiment, designed to detect a common analyte with readily available antibodies, five chips were functionalized with anti-hCG and then exposed to different concentrations of hCG in 50% serum. In this case, 14 sensors were measured per chip (Fig. 2*C*).

real-time, with an update rate of 64 data points every 5 s. Some of the sensors are covered with epoxy and used to record an electronic reference signal, so that nonbiological signal components such as temperature drift can be corrected.

Typical binding curve data (signal vs. time) from MNT-based immunoassays with multiple probes is shown in Fig. 2. The moment of MNT application is defined as t = 0. Beginning at t = 0, the signal rise reflects the binding of MNTs to the SV sensor surface in real time. As a result of the indirect labeling method used here, the real-time data contains information about the MNT-binding kinetics rather than the analyte binding kinetics, but the saturation level of an MNT-binding curve is taken as a direct measure of binding site abundance on the sensor surface, which in turn is determined by the concentration of the previously applied analyte. In addition to analyte quantification, the real-time MNT-binding curves are also used to identify and eliminate sources of error, as they help to distinguish proper (continuous, steady, saturating) from improper (discontinuous, noisy, drifting) sensor operation. For example, the fact that the signal quickly stabilizes despite an excess amount of nanotags in the solution indicates that in the absence of suitable binding sites, the nanotags do not precipitate or bind spontaneously. This is an important prerequisite for precise analyte quantification. The MNT-binding curves also reliably give the time needed for reaching signal saturation, that is, MNT-binding equilibrium. Typically the net signal gains at time t = 15 min are reported to compare different assay runs, but when few MNT-binding sites are available (due to low analyte concentration), MNT quantification can reach equilibrium in as little as 60 s.

An example of such rapid MNT quantification can be seen in Fig. 2*A*. In that experiment, a chip was functionalized with two probes (anti-TNF-α and anti-IL-1α) and one control (BSA), and the applied sample contained 0.6 pM TNF-α and 5.6 pM IL-1α. The resulting binding signals level off approximately one minute after MNT application, and the signal levels of 1.9 μV for TNF-α (8 sensors) and 4.1 μV for IL-1α (4 sensors) are significantly larger and distinct from the nonspecific signal of 0.6 μV on the BSA-functionalized control sensors.

A similarly functionalized chip was exposed to a 5.7 pM TNF-α in 50% serum, as shown in Fig. 2*B*. The resulting average signal saturates at 3.2 μV after approximately two minutes. The negative controls, consisting of both the anti-IL-1α- and BSA-functionalized sensors, report an average of 0.1 μV (range + 0.3 μV to −0.3 μV), which indicates an average signal to background ratio of 32:1 at this concentration.

To demonstrate the signal *vs*. concentration scaling relationship of an analyte in 50% serum over large changes in analyte concentrations, we ran a series of MNT-based immunoassays to detect human chorionic gonadotropin (hCG) that was spiked into 50% serum. For this test, hCG was chosen as a model analyte because reference hCG samples, high quality antibodies, and comparable commercial hCG assays are readily available. The results are shown in Fig. 2*C*. The lowest hCG concentration, 2.4 pM in 50% serum, resulted in a 14-sensor median signal of 13.6 μV (max 27, min 8.2, SD of 4.6), and for each 10-fold increase in hCG concentration, the signal approximately doubled. The results demonstrate that we can detect hCG concentrations over at least four orders of magnitude, down to the serum baseline level, which is approximately 1 pM (18). Performing the same assay in analyte-free PBS (Fig. 2*C* control assay) shows that the control signal is in a range of 2.5–3.5 μV_{rms}, which is significantly lower than the signal expected from 1 pM hCG in serum. Extrapolation of the scaling trend down to the background level indicates that our MNT-based assay can detect approximately 10 femtomolar concentrations of hCG in serum, which is better than the sensitivity of commercial ELISA kits we have compared (≈4 pM). The amount of data scatter is also comparable to commercial immunoassays and possibly the result of uneven probe molecule distribution, which is a common artifact in spotted microarrays (19). The higher signal and background levels of Fig. 2C (when compared to Fig. 2 A and B) were achieved by successively adsorbing not one but three layers of nanotags, that is, by a means of *in situ* nanotag amplification (see methods). The nanotag amplification is useful when the signal levels are so low, relative to the electrical noise of the system, that they are difficult to quantify. In such cases, nanotag amplification can often elevate the signal levels well above the quantification threshold, which leads to more consistent results. Assay results obtained this way are highly reproducible, and third party serum samples with unknown hCG concentrations have been quantified with good accuracy, simply by referencing the signal levels against the standard curve in Fig. 2*C*.

Fig. 3 shows the result of a multianalyte, multiprobe assay performed on a single chip. For this test, seven different regions of the chip were functionalized, each with one of seven capture antibodies. Additional control sensors were functionalized with BSA or epoxy. The chip was then exposed to a mixed sample containing the seven potentially recognized analytes at a concentration of 1 pg/ml each (molar concentrations 5 fM to 119 fM). Twenty-eight sensors were chosen from the sensor array to measure the signals from each of the functionalizations with some redundancy (ranging from replicate to quadruple). The initial MNT quantification was enhanced with two rounds of nanotag amplification. As seen in Fig. 3, under these conditions the minimal signal to background ratio is 4:1 and better in most cases. Sensors with identical functionalization reported very similar signal levels in most cases, but some functionalizations appear to be more sensitive than others. This is reasonable considering that the analyte affinity of each functionalization can be different. The small but nonzero signals on the BSA control sensors compared with the epoxy control could result from of a small amount of cross-reactivity, which is common in

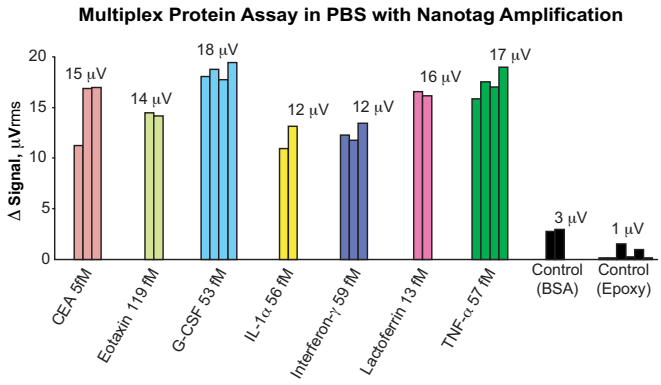

Fig. 3. Multiplex protein assay with nanotag amplification. Seven different capture antibodies were used to functionalize different regions of a chip to detect seven different protein analytes. Additionally, two sensors were functionalized with BSA and six sensors with epoxy to serve as controls. Twenty microliters of a mixed sample containing each of the seven analytes at a concentration of 1 pg/ml in PBS was then incubated on the chip for one hour. After linker incubation and initial nanotag incubation, the signal was then amplified by two additional nanotag applications. Shown are the signals from the second round of nanotag amplification. The numbers above the bars indicate the average signals for each set of sensors.

multiplex protein assays and which also depends on the matching and quality of the assay antibodies.

Discussion

Until recently most experiments were focused on proof of concept, that is, modeling and optimization of MNT-sensor interaction (16), developing the electronic platform (10), estimating the potential of MNT-based assays, for example, when compared with fluorescent assays (14), and demonstrating the principal benefits of incorporating microfluidics and MNT manipulation techniques (20). Although some efforts have been made to move these concepts into the bioanalytical arena (7–11, 13–15), there are few demonstrations of actual magnetic protein assays of either single or multiple analytes in a buffer or serum sample. In particular, multiple analytes require sophisticated biochemistry as well as control sensors on a single chip to ascertain sensitivity and selectivity at the same time. Selectivity is particularly challenging to achieve in multiplex protein assays and assays involving actual blood serum, where unexpected cross-reactivity can occur much more readily than in DNA hybridization assays. Our experiments demonstrate that MNT-based biomolecular assays are capable of fast and sensitive multiplex protein detection involving real-world serum samples.

Another significant advance reported here concerns the magnetic and kinetic properties of the MNTs. Magnetic analyte quantification has been demonstrated for DNA detection and has typically required large magnetic labels that range in size from approximately 250 nm to 3 μm (11, 12, 14, 21). These μm-sized labels are not optimal for biomolecular assays—they diffuse slowly, are prone to magnetic interaction and subsequent precipitation, and are very bulky compared with the analyte molecules. To overcome these limitations, we have focused on detecting nanometer sized MNTs such as commercially available 50-nm MACS MNTs (see methods), which have a very small magnetic signature but which exhibit long term suspension stability and excellent binding selectivity. To enhance the sensitivity of our assay, the passivation of the SV sensors in this article has been thinned to an unprecedented 30 nm. The resulting sensitivity allows us to reliably detect minute magnetic signatures, such as from MACS MNTs, provided that they are in the immediate proximity of the sensor. By combining small magnetic moment MNTs with very sensitive proximity detection, our sensors primarily detect MNTs that are bound to the sensor surface. If unbound MNTs are stable in suspension, then the signal contribution from these extraneous unbound MNTs is negligible, and washing steps, which are typically required to remove unbound signal-generating labels, can be omitted. In practice, this suppression of unbound labels means that the true amount of currently bound nanotags can be observed in real-time, and that negative control sensors experience no signal shift and return during nanotag application and removal. Simple one-step homogeneous assays with no washing steps are thus a possibility, which would further enhance the use of this technology in clinical applications.

Our 50-nm MNT-based assay overcomes all previous detection shortcomings and presents the most sensitive magnetic detection method for protein arrays to date. With carefully screened antibodies, the sensitivity and selectivity of our MNT-based analyte quantification method is already sufficient for clinically relevant protein detection in real world serum samples, and multiplex protein detection can be readily performed with this method. Individual sensor microspotting (see SI) will allow the accommodation and simultaneous measurement of up to 64 different probes on a chip of the current generation. We expect that significant improvements can also be made on the sensor, for example, using magnetic tunnel junction sensors (9, 22) instead of spin valves, and by using sensors with narrower segments (16) (see SI). In the near future, capture agents with higher affinity, and similarly small but higher magnetic moment MNTs are all expected to enhance the analytic sensitivity of MNT-based assays further. We believe that the demonstrated capability of detecting multiple biomarkers on a single chip, combined with sensitivity, scalability, and ease of use, make this protein assay method a strong contender for portable multiplexed molecular diagnostics at or near point-of-care. It is also notable that MNT-based analyte quantification with SV sensors has several advantages over other methods: The sensors are easy to fabricate, pH-insensitive, and with no "bleaching" of MNTs and no magnetic background from bio-systems, MNT-based assays produce signals that are exceptionally stable even during drastic changes of experimental conditions, such as wet to dry transitions. MNT-based analyte quantification can also be conveniently combined with magnetic separation techniques, which should lead to further assay simplifications. For example, analyte extraction and the first round of molecular amplification have already been combined into a single magnetic separation step to achieve an ultrasensitive protein detection (23), which, however, still relies on optical analyte quantification to obtain the final result. All of these positive attributes will make it easier to translate MNT-based protein assays to clinical settings.

Materials and Methods

Chip Fabrication. On silicon wafers with 150-μm thermal oxide, a spin valve film with a layer sequence similar to that of hard disk drives read heads was patterned by ion milling into individual sensors (9), each consisting of 32 linear segments of 1.5 $\times$ 100 μm connected in series and arranged to cover an area of 100 $\times$ 100 μm^2 (see SI). Each sensor had a nominal resistance of 40 kΩ and a maximum magnetoresistance of 12%. Corrosion resistant leads (Ta 5/Au 300/Ta 5) nm were sputter deposited and patterned by lift-off. As suggested elsewhere (24), the sensors were passivated with a tri-layer oxide (SiO_2 10/Si3N4 10/SiO_2 10) nm that was deposited at room temperature by ion beam sputter deposition. The leads were passivated with an additional tri-layer oxide (SiO_2 100/Si_3N_4 100/SiO_2 100) nm. A two-component epoxy (EP5340, Eager Plastics) was used to assemble the chip and reagent well (Tygon tubing, 1/4'' ID $\times$ 3/8'' OD, 6 mm long) on the ceramic 84-pin chip carrier (LCC08423, Spectrum Semiconductor Materials). A 0.5 mm layer of the same epoxy was used to mask some of the sensors (see SI). The masked sensors, no longer able to detect nanotag binding, would serve as electrical signal references (see *Methods - Electronics*).

Surface Preparation. The assembled chips were thoroughly washed with acetone, methanol, isopropanol, and de-ionized water. A 10-min UV ozone treatment (UVO Cleaner Model 42, Jelight) was used to remove organic residues. To form the base layer of the biofunctionalization, a 2% solution of polyethyleneimine (PEI, CAS 9002–98-6, Sigma-Aldrich) in deionized water was applied to the chip surface for 2 min. The chips were then rinsed with deionized water and then baked at 150°C for 5 min to solidify the adsorbed PEI.

Multiplex Protein Assays. For multiplex experiments with three distinct probes, the probes (anti-IL-1α and anti-TNF-α at 500 μg/ml, and BSA at 1%, i.e., 10 mg/ml) were manually deposited with a pipette in the form of 0.2-μl droplets onto selected sites, each covering several sensors, of a single chip. For multiplex experiments with eight distinct capture probes, the probes (anti-IL-1α, anti-TNF-α, anti-CEA, anti-G-CSF, anti-IFN-γ, anti-lactoferrin, anti-eotaxin, at 1%) were robotically spotted in the form of 2-nL droplets onto individual sensors. Additional control sensors were functionalized with epoxy resin. The spotted chips were incubated overnight at 4°C in a humidifier. The chips were then rinsed twice with blocking buffer (1% BSA and 0.2% Tween 20 in PBS), and further blocked with the same buffer for 60 min at room temperature to reduce nonspecific surface binding sites. Samples consisting of multiple proteins in the same solution were then prepared by mixing several analytes (TNF-α; IL-10; IL-1α; G-CSF; lactoferrin; CEA; eotaxin; and IFN-γ) to the desired concentrations in either PBS buffer or in 50% human serum (balance PBS). Twenty microliters of this sample solution were pipetted into the reagent well of a chip and incubated for 1 h at room temperature, so that all of the sensors on the chip were exposed to the same multiprotein sample solution. Subsequently, the chip was rinsed twice with rinsing buffer (0.1% BSA and 0.2% Tween 20 in PBS). A multiplex linker antibody solution was prepared consisting of multiple biotinylated antibodies, one type for each potential analyte, at a concentration of 2 μg/ml in PBS. Twenty microliters of this linker antibody solution were incubated in the reagent well of the chip for 1 h at room temperature. With the linker solution still in place, the chips were then transferred over to the measuring station for MNT-based analyte quantification.

hCG Assays. All chips were uniformly functionalized with a single capture probe, anti-hCG at 1 mg/ml, incubated overnight at 4°C, then rinsed twice with blocking buffer. Pure serum samples spiked with hCG to 2.5, 25, 250, and 2,500 IU/L were supplied by the US National Cancer Institute and diluted 1:1 with PBS buffer. Analyte incubation was 1 h, and linker antibody at 5 μg/ml in PBS, was incubated for 90 min. With the linker solution still in place, the chips were then transferred over to the measuring station for MNT-based analyte quantification. The concentrations of hCG after dilution with PBS have been converted by using 1 IU/L = 1.9 pM (25, 26).

MNT-Based Analyte Quantification. To remove the linker antibody solution and to confirm signal baseline stability, the chips were rinsed with MNT-free PBS buffer several times. Although the associated wet/dry transitions did occasionally shift the baseline slightly, these shifts were reversible and usually negligible compared with the signals of interest. The absolute signal level on contact with MNT-free buffer was taken to be zero. The MNT-free buffer solution was then aspirated from the well and replaced with 50 μl of streptavidin-coated MNT stock solution (MACS 130–048-102, Miltenyi Biotec; for additional details, see SI). The nanotag solution was incubated without stirring for the next 20 min at room temperature. The signal levels at the end of this 20-min nanotag incubation time were taken as the final result of the assay.

Optional Nanotag Amplification. At the end of the initial 20-min MNT incubation period, the well was rinsed five times with PBS, and then refilled with 50 μl of the biotinylated linker antibody solution. This solution was incubated for five minutes, attaching biotinylated antibodies to the already adsorbed MNTs. Because these linker antibodies can have multiple biotin sites, binding sites for additional MNTs were created this way on the existing MNTs. After five minutes, the solution was aspirated, the well rinsed five times with PBS, and 50 μl of MNT stock solution were added, resulting in the generation of an additional MNT binding signal. This amplified the signal levels by a factor of approximately 2$\times$ with each iteration (see SI for additional data).

Electronics. An alternating current of 7 μA_{rms} at 500 Hz was applied to each sensor. An alternating in-plane tickling field of 80 Oe_{rms} at 208 Hz was applied perpendicular to the sensor segments to establish a magnetic signal baseline, which is minimally perturbed in the vicinity of any nanotags. This perturbation of baseline signal is our net signal. A steady bias field of 50 Oe was also applied along the longitudinal direction of the sensor segments to facilitate a coherent (low noise) rotation of the magnetic domains of the sensor in response to the 208-Hz tickling field. The signal level was measured by performing a fast Fourier transform of the voltage across each sensor once per second and recording the magnitude of the (amplitude modulation generated) 708-Hz spectral component, which in this setup is primarily a measure of the tickling field strength in the immediate vicinity of the sensor. To reduce the common mode and sensor drift, every functionalized sensor was measured differentially against a reference sensor, that is, against a sensor that was covered with a layer of epoxy thick enough to positively prevent any MNT detection. Additional details of this measurement setup are described elsewhere (27).

ACKNOWLEDGMENTS. We thank the Stanford Nanofabrication Facility where the prototype chips were developed. This work was supported in part by National Institutes of Health Grants 1U54CA119367–01, PO1-HG000205, N43C0–2007-00030, and R43AI072800 and the Defense Advanced Research Projects Agency/Navy Grant N00014–02-1–0807.

1. Kingsmore SP (2006) Multiplexed protein measurement: Technologies and applications of protein and antibody arrays. *Nat Rev Drug Discov* 5:310–320.
2. Sawyers CL (2008) The cancer biomarker problem. *Nature* 452:548–552.
3. Schena M, Shalon D, Davis RW, Brown PO (1995) Quantitative monitoring of gene expression patterns with a complementary DNA microarray. *Science* 270:467–470.
4. Puntes VF, Krishnan K, Alivisatos P (2001) Nanocrystals size and shape control: The case of Co. *Science* 291:2115–2117.
5. Sun SH, *et al.* (2004) Monodisperse MFe_2O_4 (M=Fe, Co, Mn) nanotags. *J Am Chem Soc* 126:273–279.
6. Uhlen M (1989) Magnetic separation of DNA. *Nature* 340:733–734.
7. Edelstein RL, *et al.* (2000) The BARC biosensor applied to the detection of biological warfare agents. *Biosens Bioelectron* 14:805–813.
8. Xu L, *et al.* (2008) Giant magnetoresistive biochip for DNA detection and HPV genotyping. *Biosens Bioelectron* 24:99–103.
9. Shen W, *et al.* (2008) Detection of DNA labeled with magnetic nanoparticles using MgO-based magnetic tunnel junction sensors. *J Appl Phys* 103:07A306.
10. Boer BM, Kahlman JAHM, Jansen TPGH, Duric H, Veen J (2006) An integrated and sensitive detection platform for magneto-resistive biosensors. *Biosens Bioelectron* 22:2366–2370.
11. Baselt DR, *et al.* (1998) A biosensor based on magnetoresistance technology. *Biosens Bioelectron* 13:731–739.
12. Li G, *et al.* (2003) Detection of single micron-sized magnetic bead and magnetic nanoparticles using spin valve sensors for biological applications. *J Appl Phys* 93:7557–7559.
13. Graham DL, Ferreira H, Bernardo J, Freitas PP, Cabral JMS (2002) Single magnetic microsphere placement and detection on-chip using current line designs with integrated spin valve sensors: Biotechnological applications. *J Appl Phys* 91:7786–7788.
14. Schotter J, *et al.* (2004) Comparison of a prototype magnetoresistive biosensor to standard fluorescent DNA detection. *Biosens Bioelectron* 19:1149–1156.
15. Millen RL, Kawaguchi T, Granger MC, Porter MC, Tondra M (2005) Giant magnetoresistive sensors and superparamagnetic nanotags: A chip-scale detection strategy for immunosorbent assays. *Anal Chem* 77:6581–6587.
16. Li G, *et al.* (2006) Spin valve sensors for ultrasensitive detection of superparamagnetic nanotags for biological applications. *Sens Actuators A Phys* 126:98–106.
17. Sandhu M (2007) Biosensing: New probes offer much faster results. *Nat Nanotechnol* 2:746–748.
18. Korhonen J, Alfthan H, Ylostalo P, Veldhuis J, Stenman UH (1997) Disappearance of human chorionic gonadotropin and its alpha- and beta-subunits after term pregnancy. *Clin Chem* 43:2155–2163.
19. Pappaert K, Ottevaere H, Thienpont H, Van Hummelen P, Desmet G (2007) Diffusion limitation: A possible source for the occurrence of doughnut patterns on DNA microarrays. *BioTechniques* 41:609–616.
20. Janssen XJA, Ijzendoorn LJ, Prins MWJ (2007) On-chip manipulation and detection of magnetic particles for functional biosensors. *Biosens Bioelectron* 23:388–838.
21. Sandhu A, Handa F (2005) Practical hall sensors for biomedical instrumentation *IEEE Trans Magn* 41:4123–4127.
22. Yuasa S, Nagahama T, Fukushima A, Suzuki Y, Ando K (2004) Giant room-temperature magnetoresistance in single-crystal Fe/MgO/Fe magnetic tunnel junctions. *Nat Mater* 3:868–871.
23. Oh BK, Nam JM, Lee SW, Mirkin CA (2006) A fluorophore-based bio-barcode amplification assay for proteins. *Small* 2:103–108.
24. Schmitt G, *et al.* (1999) Passivation and corrosion of microelectrode arrays. *Electrochim Acta* 44:3865–3883.
25. Birken S, *et al.* (2003) Preparation and characterization of new WHO Reference Reagents for human chorionic gonadotropin and metabolites. *Clin Chem* 49:144–154.
26. Sturgeon CM, Ellis AR (2007) Standardization of FSH, LH and hCG - Current position and future prospects. *Mol Cell Endocrinol* 260:301–309.
27. Han SJ, Xu L, Wilson RJ, Wang SX (2006) A novel zero-drift detection method for highly sensitive GMR biochips. *IEEE Trans Magn* 42:3560–3562.